

Spatial tuning of laser emission in a dye-doped cholesteric liquid crystal wedge cell

Mi-Yun Jeong, Hyunhee Choi, and J. W. Wu

Citation: *Appl. Phys. Lett.* **92**, 051108 (2008); doi: 10.1063/1.2841820

View online: <http://dx.doi.org/10.1063/1.2841820>

View Table of Contents: <http://aip.scitation.org/toc/apl/92/5>

Published by the [American Institute of Physics](#)



**THE WORLD'S RESOURCE FOR
VARIABLE TEMPERATURE
SOLID STATE CHARACTERIZATION**



OPTICAL STUDIES SYSTEMS



SEEBECK STUDIES SYSTEMS



MICROPROBE STATIONS



HALL EFFECT STUDY SYSTEMS AND MAGNETS



WWW.MMR-TECH.COM

Spatial tuning of laser emission in a dye-doped cholesteric liquid crystal wedge cell

Mi-Yun Jeong, Hyunhee Choi, and J. W. Wu^{a)}

Department of Physics and Division of Nano Sciences, Ewha Womans University, Seoul 120-750, Korea

(Received 27 November 2007; accepted 20 January 2008; published online 6 February 2008)

Spatial tuning of lasing wavelength in a dye-doped cholesteric liquid crystal wedge cell is demonstrated. The wedge cell possesses a series of dislocation lines along the wedge direction. In the lasing operation, we find that the lasing wavelength is continuously tuned in the region between two dislocation lines, while the lasing wavelength jumps when crossing the dislocation lines. The observed one-dimensional spatial continuous tuning is attributed to the presence of a gradient in the cholesteric helical pitch, while the laser wavelength jumping originates from the pitch jump owing to a change in the number of half-turns of the cholesteric helix. © 2008 American Institute of Physics. [DOI: 10.1063/1.2841820]

After Kopp *et al.*¹ reported a lasing operation in a dye-doped cholesteric liquid crystal (CLC), the research has been focused on how to implement the tunability of the laser operation wavelength. The concentration and helical twisting power of chiral dopants in the CLC determine the CLC pitch, which subsequently determines the spectra of the stopband. The structure property of liquid crystal is easily controlled by an external influence such as temperature, mechanical stress, and electric field, which have been utilized to tune the lasing wavelength.² While the temperature tuning involves both the change in the refractive index and the pitch,³ the mechanical stress affects the pitch variation only.⁴

As a further development to attain the laser wavelength tunability in a single device of the CLC laser, the one-dimensional (1D) spatial tunability has been achieved by introducing a temperature gradient in a CLC,⁵ an UV cured-fixed temperature gradient in a cholesteric polymer,⁶ and a chiral dopant concentration gradient⁷ in a CLC. On the other hand, it is well known that the equilibrium structure of a CLC confined within a finite volume is determined by bulk elasticity and boundary effects, such as surface tension and surface anchoring.⁸ In a geometrically deformed cell structure such as a Cano wedge cell, there appear dislocations in order to satisfy the boundary condition. In fact, Cano lines observed in a wedge design of a CLC cell are dislocation lines which form between two regions of different numbers of half-turns of the cholesteric helical pitch, and a wedge cell has been utilized to determine the pitch of a CLC.⁹ In between two Cano lines, the pitch of CLC goes through a gradual change, providing a gradient laser cavity length for a CLC lasing. In this letter, we report on the 1D spatial tuning of lasing wavelength in a wedge CLC cell.

The CLC sample is composed of a nematic ZLI2293 with the chiral dopant S811 (Merk), and the laser dye 4-dicyanomethylene-2-methyl-6-p-dimethylaminostyryl-4H-pyran (DCM) was mixed in 0.5 wt %. SE-5291 polyimide is employed for alignment layer, which has a typical pretilt angle of 6°–7°. The dye-doped CLC sample is in the form of a left-handed helix. The wedge cell was prepared by employing two spacers with different thicknesses, and we could easily achieve a spatial gradient corresponding to the thickness

change of $\approx 0.1 \mu\text{m}$ over the distance of 1.0 cm. Figure 1(a) shows the photographic picture of the fabricated cell exhibiting a series of Cano dislocation lines. The typical spacing between two adjacent dislocation lines is $400 \mu\text{m}$, which is determined by the spatial gradient and the helical rotating power. As shown in Fig. 1(b), the number n of half-turns is related to the pitch at the given dislocation line such that $(n-1)p_2/2 = np_1/2$ and $np_2/2 = (n+1)p_1/2$ with $p_1 < p_2$. In the region between two dislocation lines, the pitch varies continuously from p_1 to p_2 as moving along the $+x$ direction.

We examined the stopband structure of one region by measuring the optical reflection spectra. A broad stopband possessing 50% reflection was observed in the spectral range of 570–630 nm, as shown in Fig. 2 as the black curve. For a CLC structure forming a given handedness helix, the selective reflection occurs for the circularly polarized light possessing the same handedness as that of the CLC. The selective reflection spectra can be calculated from the analysis of light propagation in a CLC structure by adopting the 4×4 matrix method developed by Berreman.^{10,11} Once the simulated reflection spectra are obtained, the density of photonic states is calculated by following the procedure reported by Bendickson *et al.*¹² The theoretical calculation of the density of mode spectra is plotted as the dotted curve.

A second harmonic generation from a Q -switched neodymium doped yttrium aluminum garnet laser (pulse width of 10 ns) was employed as the optical pump with a typical intensity of several MW/cm^2 . The pump beam was linearly polarized. In the inset, the lasing intensity is plotted as a function of the pump beam intensity. We find that there

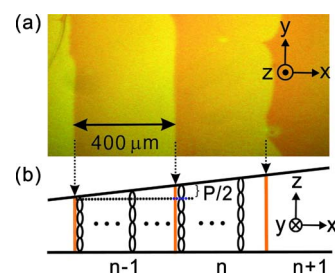


FIG. 1. (Color online) (a) Photographic picture of the sample cell. Cano dislocation lines are observed with a typical spacing of 400 nm. (b) The schematic diagram of the wedge cell with the half-turns of helical pitch.

^{a)}Electronic mail: jwwu@ewha.ac.kr.

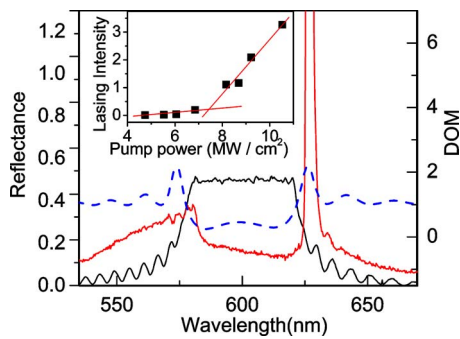


FIG. 2. (Color online) The optical reflection spectra of the stopband (black curve), the fluorescence spectra with the lasing peak (red curve), and the density of mode spectra (dotted curve) are shown. The inset shows the lasing intensity as a function of the pump beam intensity.

exists a threshold behavior characteristic of the laser operation. The fluorescence from the DCM laser dye and the lasing spectra are shown as the red curve. The polarization of the fluorescence and laser light wave were examined by a combination of polarizers and wave plates. While the fluorescent light placed outside the stopband is unpolarized, the laser light is left-circularly polarized. In the CLC lasing, the fluorescence from the laser dye is suppressed inside the stopband, while the enhanced density of modes in the band edge of the stopband allows for a multiple reflection in the cholesteric helix resulting in a laser operation. We find that the lasing operation occurs at the longer wavelength band edge of the stopband.

Near the bandgap edges of the left-handed helix CLC, the left-circularly polarized light experiences multiple reflections. The interference of the forward- and backward-propagating light results in two standing waves. The mode structure of two standing waves can be obtained from the analysis of energy-momentum dispersion relation, and it is known that two standing waves are linearly polarized with the polarization direction parallel to the extraordinary (ordinary) axis at the longer (shorter) wavelength band edge, called the in-phase (out-of-phase) standing wave.^{9,13} In other words, the polarization direction of the resulting standing wave forms a helix, and the electric field of the in-phase standing wave oscillates along the nematic director. Since the linearly shaped rodlike DCM molecules prefer to get aligned parallel to the nematic director, the CLC laser cavity in the longer wavelength band edge of the stopband is much more efficient in amplifying the stimulated emission of fluorescence. We note that the standing wave cavity structure of the CLC laser is more efficient than that of a linear cavity in exploiting the fluorescent light for lasing operation since no spatial hole burning is present.

Once the lasing operation is identified, we examined the spatial tunability of the lasing peak wavelength by translating the pump beam position on the dye-doped CLC cell along the x direction. In Fig. 3, the spectra of both lasing wavelength and stopband are shown simultaneously. As the pump beam position changes from $x=1.225$ mm to $x=1.675$ mm, the peak of lasing wavelength is tuned from 617 to 626 nm in the region between two dislocation lines. Since the pitch of CLC dilates continuously, the lasing wavelength moves to the longer wavelength. In Fig. 4 is plotted the peak lasing wavelength as a function of the position in the wedge cell. We observe a jump in the lasing wavelength when crossing the dislocation line, and at the dislocation

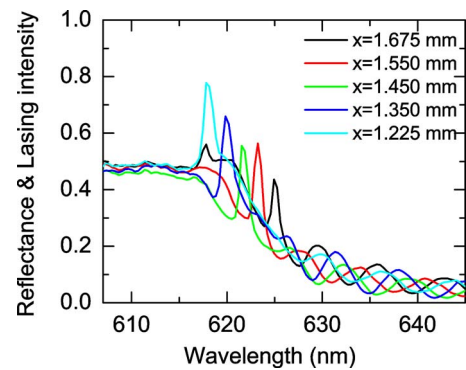


FIG. 3. (Color online) The spectra of both lasing wavelength and stopband are shown simultaneously as the pump beam position is translated along the x -axis direction.

line, there occur two simultaneous lasing corresponding to the original pitch p_1 and the maximally dilated pitch p_2 .

Now let us turn to the analysis of the lasing wavelength tuning. Huang *et al.* reported on the spatial tuning of the lasing wavelength by adopting a CLC structure with a built-in gradient.^{5,6} In Ref. 5, a CLC cell possessing a temperature gradient was fabricated based on the combined effect of temperature-dependent chiral agent solubility and birefringence. There occurs shift of λ_{edge} to a shorter wavelength upon temperature increase, owing to the higher solubility and subsequent helical pitch reduction. With the temperature gradient maintained by placing the cell between a hot plate and the open air, a spatial tunability of the lasing wavelength was achieved. In the 10 μm thick CLC cell structure with two parallel glass substrates, a continuous gradient is built in, resulting in a continuous tuning of lasing wavelength.

In Ref. 6, on the other hand, the temperature gradient of the chiral agent solubility is fixed by UV curing the cholesteric polymer film. In the sense that the CLC cell is of a standalone type, it is similar to our sample. The difference lies in that the sample in Ref. 6 is a parallel cell with an UV-fixed built-in gradient formed by a temperature-dependent chiral agent solubility, while our sample is a wedge cell with no temperature gradient built in. The spatial tuning of the lasing wavelength in the wedge cell is from the pitch variation occurring between two dislocation lines coming from the competition between the torques on the director originating from the bulk and the surface anchoring. Along the $+x$ -axis direction starting from a dislocation line, the surface anchoring is still dominant compared with the bulk

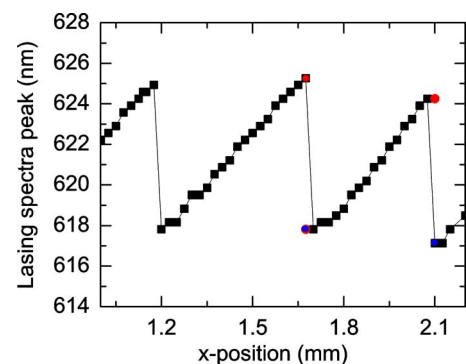


FIG. 4. (Color online) The peak lasing wavelength is plotted as a function of the pump beam position on the wedge cell.

torque, resulting in the pitch elongation, subsequently a longer lasing wavelength. Approaching the next dislocation line, the bulk torque gets dominant causing the LC director slippage on the alignment surface, resulting in the change of the number of half-turns by 1. This incurs an abrupt change in the pitch, subsequently a jump in the lasing wavelength to a shorter wavelength corresponding to the natural, undilated helical pitch.

A similar jump in the lasing wavelength has been observed in the work on the CLC laser as an optic fiber-based temperature sensor by Moreira *et al.*³ As can be seen in Fig. 3 of Ref. 3, upon temperature increase, the lasing wavelength moves toward a shorter wavelength and goes through a jump in the lasing wavelength. The temperature dependence of the twist elastic constant K_{22} can be one possible mechanism for the helix wavenumber variation, providing the temperature tunability of the lasing wavelength.¹⁴ The jump in the lasing wavelength, on the other hand, is attributed to the abrupt change in the nematic director's orientation, resulting in the jump of the helical pitch. One possible mechanism of the temperature induced jump of the helix pitch in a spatially bounded planar layer of a CLC is related to transitions between the ground states of different configuration curves corresponding to a topologically nonequivalent configuration, which requires participation of dislocation lines.¹⁴

In contrast, the presence of dislocation lines in the Cano wedge cell is understood in terms of defects in the elastic liquid crystal.¹⁵ Based on the fluorescence confocal polarizing microscopy measurement, the three-dimensional director structures of defects have been analyzed, which were described by employing the elastic model of defect structures in cholesteric Cano wedge.⁸ For a Cano wedge cell with thickness greater than the critical thickness, the dislocation line is stable at equilibrium, which is the case for our sample geometry.

In summary, a spatial tuning of lasing wavelength is demonstrated in a dye-doped cholesteric liquid crystal wedge cell. Owing to the helical pitch dilation in the region between two Cano dislocation lines, the lasing wavelength is continuously tuned. When crossing the dislocation lines, there occurs a jump in the lasing wavelength, which is attributed to a change in the number of half-turns of the cholesteric helix. The spatial tuning of laser emission lines in the wedge cell provides a new design of a single optical element of spatially tunable lasing operation.

This work is supported by the Seoul Research and Business Development Program (10816), ABRL program at Ewha Womans University, as well as by the Korea Research Foundation (Grant No. KRF-2006-005-J04001).

¹V. I. Kopp, B. Fan, H. K. M. Vithana, and A. Z. Genack, *Opt. Lett.* **23**, 1707 (1998).

²A. D. Forda, S. M. Morrisa, and H. J. Colesa, *Mater. Today* **9**, 36 (2006) and references therein.

³M. F. Moreira, I. C. S. Carvalho, W. Cao, C. Bailey, B. Taheri, and P. Palffy-Muhoray, *Appl. Phys. Lett.* **85**, 2691 (2004).

⁴H. Finkelmann, S. T. Kim, A. Muaoz, P. Palffy-Muhoray, and B. Taheri, *Adv. Mater. (Weinheim, Ger.)* **13**, 1069 (2001).

⁵Y. Huang, Y. Zhou, and S.-T. Wu, *Appl. Phys. Lett.* **88**, 011107 (2006).

⁶Y. Huang, L.-P. Chen, C. Doyle, Y. Zhou, and S.-T. Wu, *Appl. Phys. Lett.* **89**, 111106 (2006).

⁷A. Chanishvili, G. Chilaya, G. Petriashvili, R. Barberi, R. Bartolino, G. Cipparrone, A. Mazzulla, and L. Oriol, *Adv. Mater. (Weinheim, Ger.)* **16**, 791 (2004).

⁸I. Smalyukh and O. D. Lavrentovich, *Phys. Rev. E* **66**, 051703 (2002).

⁹P. G. De Gennes and J. Prost, *The Physics of Liquid Crystals* (Clarendon, Oxford, 1993).

¹⁰D. W. Berreman, *J. Opt. Soc. Am.* **62**, 502 (1972).

¹¹D. W. Berreman, *J. Opt. Soc. Am.* **63**, 1374 (1973).

¹²J. M. Bendickson, J. P. Dowling, and M. Scalora, *Phys. Rev. E* **53**, 4107 (1996).

¹³M. Ozaki, Y. Matsuhisa, H. Yoshida, R. Ozaki, and A. Fujii, *Phys. Status Solidi A* **204**, 3777 (2007).

¹⁴S. P. Palto, *JETP* **94**, 260 (2002).

¹⁵M. Kleman, *Rep. Prog. Phys.* **52**, 555 (1989).